# Multiaxial Fatigue Criteria and Durability of Titanium Compressor Disks in Low- and Very-high-cycle Fatigue Modes

**Nikolay Burago and Ilia Nikitin**

**Abstract** Life duration for titanium disks of low temperature part of compressor aero-engine D30-Ku is investigated. Several criteria and models are tested under conditions of low-cycle fatigue (LCF) and very-high-cycle fatigue (VHCF). Parameters of the criteria and models are determined from uniaxial fatigue tests for titanium alloy VT3-1. Stress-strain state of disks and blades is calculated taking into account cyclic centrifugal, aerodynamic, contact loads and blade vibrations. Calculated stresses and strains are used as input data for multiaxial models of LCF and VHCF regimes. Location and scales of fracture as well as time to fracture are calculated. The results of calculations are in good agreement with observations during engine exploitation and correspond to data of fractographic investigations of damaged disks.

**Keywords** Fracture and damage · Fatigue criteria

**Mathematical Subject Classification:** 74R20

## 1 Introduction

In this paper we consider the problem of determining the duration of safe operation of structures. In experiments [1] it is shown that under the action of cyclic loads after several millions or billions of cycles the material may be damaged even if during this time only small elastic deformations were observed and in the material there were no signs of macroscopic defects. To date, several phenomenological models of fatigue failure have been developed [2, 5–9, 11–13], generalizing the experimental

N. Burago (✉)
Ishlinski Institute for Problems in Mechanics of RAS, Vernadskogo 101, Block 1, 119526 Moscow, Russia
e-mail: burago@ipmnet.ru

I. Nikitin
Institute for Computer Aided Design of RAS, 19/18 2nd Brestskaya Street, 123056 Moscow, Russia
e-mail: i_nikitin@list.ru



P. Neittaanmäki et al. (eds.), *Mathematical Modeling and Optimization of Complex Structures*, Computational Methods in Applied Sciences 40,
DOI 10.1007/978-3-319-23564-6_8

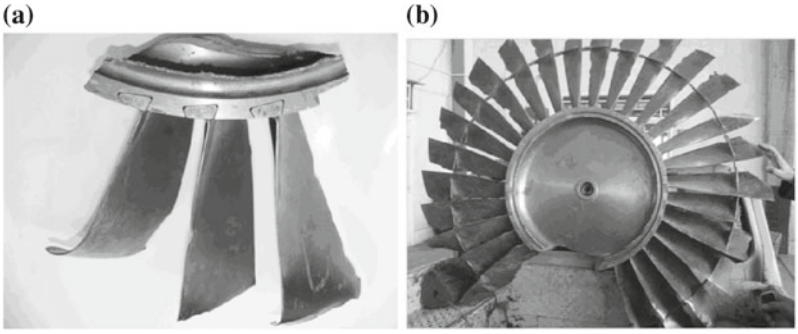


**Fig. 1** Fracture in disks for compressor of aero engines D30-KU-154

data for the case of a multiaxial stress-strain state. To determine the safe operation life of structures for such models it is sufficient calculate the stress-strain state using the linear theory of elasticity. Available models of fatigue failure are divided into three groups, the first of which is based on the criteria of stress state [5, 7, 11], the second group is based on criteria for strain state [2, 6, 12], and third group is based on the calculation of the kinetics of damage [8]. The physical nature of damage in the material structure under the action of cyclic loads, which is investigated in e.g. [1, 10], is still an active topic of study.

Fatigue fracture of disks of gas turbine engines (GTE) is a well-known phenomenon [10]. The gas turbine engines are subjected to various cyclic loads. The cycles of "take-off-flight-landing" correspond to low cycle fatigue. The presence of small vibrations with $R = \sigma_{\min}/\sigma_{\max} > 0.8$ corresponds to very high cycle fatigue.

It is demonstrated that such additional loads can essentially alter the picture of damage accumulation in service. There were several unpredicted cases of damage to titanium rotor disks in the low pressure compressor stage in the D30-KU-154 engine (Fig. 1). The fatigue failures may take place earlier than in accordance with the LCF criteria, and that is why a new numerical approach is developed here in order to estimate and to compare life duration predictions not only for the LCF but also for the VHCF regimes.

The finite element model for the disk with blades under consideration is developed in [3] and the 3D stress-strain state is analyzed there taking into account centrifugal and aerodynamic loads, contact and vibration loads. Aero-elastic effects due to mutual influence of aerodynamic loads and structural shape changes are also taken into account.

It is assumed that during the flight cycle the maximum values of stresses and strains correspond to the aircraft flight velocity of 200 m/s and the disk rotation frequency of 3000 rpm. It is assumed that during many years of safe exploitation the disks are subjected only to elastic deformations and do not contain cracks. Our first goal is to calculate disk life duration as the limiting number of cycles to failure and to detect the location of failure using fatigue criteria [2, 4–9, 11–13] for LCF regime of cyclic loading. The results are compared to available in-flight data.

Our second goal is to study the VHCF regime of cyclic loading due to additional action of high frequency axial vibrations of blade shroud ring. The maximum vibration amplitude is assumed to be at a disk rotation frequency of 3000 rpm. Evaluations of life duration are presented in terms of the number of vibration cycles according to various VHCF criteria.

Until now, in the literature there are no experimental data and theoretical multiaxial models applicable to the considered material (titanium alloy VT3-1) for VHCF regime. Therefore the known multiaxial LCF criteria are generalized here and are applied to study the VHCF regime. The generalization is performed using similarity of the left and right branches of bimodal fatigue curves. The values of parameters for generalized criteria are determined using the few available experimental data found for VHCF regime.

There are no other publications on the life duration estimates for three-dimensional structure in VHCF regime in scientific literature yet. The calculated results for the low-cycle and very-high-cycle fatigue are compared. It is found that in the life duration estimates are close to each other. That is why the VHCF mechanism should be taken into account in the resource estimates of GTE.

## 2 Computational Model of Contact Structure "Disk and Blades"

The application of finite element method for contact structure disk and blades is described in [3]. The three-dimensional stress-strain state of the contact system of the compressor disk and blades (Fig. 2) is numerically analyzed using finite-element method. The distributed aerodynamic loads are approximated using analytical methods based on modification of classical solutions to the problem of flow about a lattice of plates at arbitrary angle of attack. The solution of aerodynamic problem is obtained using theory of complex variable methods and the isolated profile hypothesis with the blade deformable shape changes taken into account [3]. The combined action of centrifugal, aerodynamic and contact loads is taken into account. First, stress-strain state is calculated for the full computational model "disk with 22 blades" (Fig. 2a) using a rough grid with a number of elements of about $10^5$. Then, the solution obtained from the calculation of the full model is used to move the boundary conditions onto the sides of the disk sector with a single blade (Fig. 2b), which is calculated using the refined grid with the same number of finite elements of about $10^5$, which is quite acceptable for calculations on a personal computer. Calculated stresses and strains are used in LCF and VHCF models for life duration estimations.

Extended numerical model is used for VHCF analysis taking into account low-amplitude axial vibrations of shroud ring. The vibrations cause axial displacements of the shroud ring. The vibrations along the ring take the form of 12–16 half waves. For the disc-blade sector calculation it was assumed that the displacement of right side of shroud ring is equal to zero and that the displacement of its left side varies

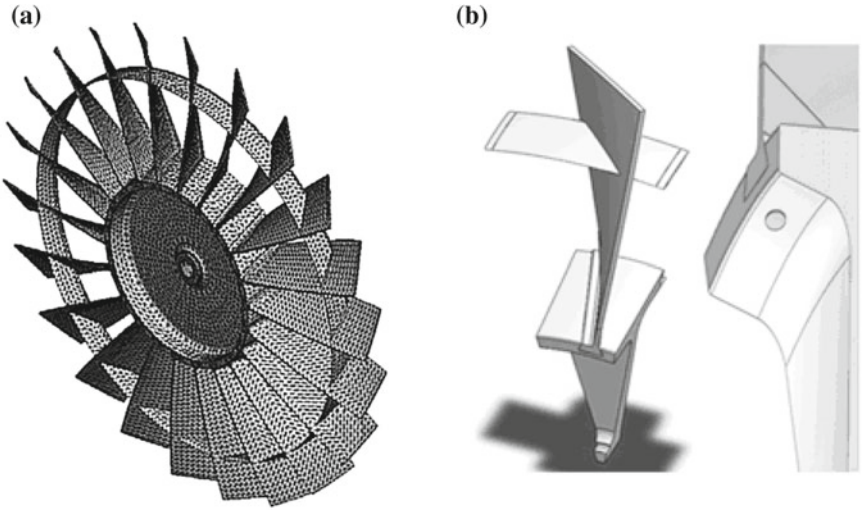


**Fig. 2** The contact system of the compressor disk and blades: **a** disk-blades contact structure, **b** disk sector with blade and part of shroud ring

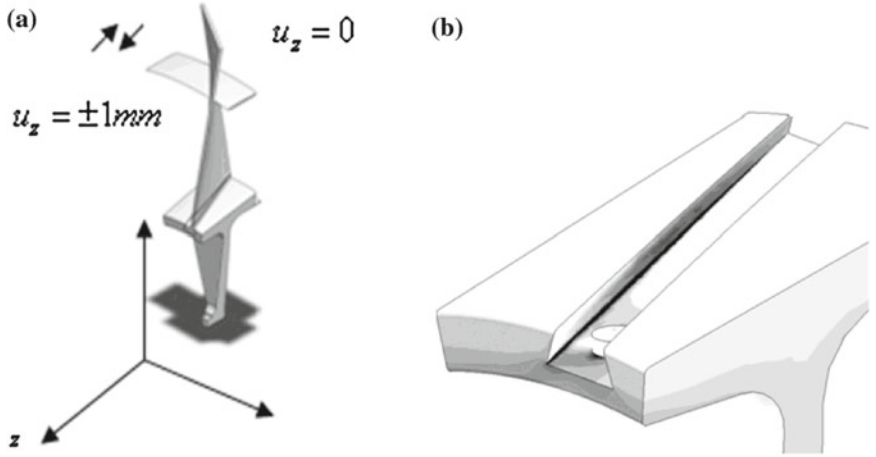


**Fig. 3** The contact system of the compressor disk and blades: **a** schematic for vibration analysis, **b** the slot of dovetail-type connection

in the range the maximal vibration amplitude of $\pm 1$ mm (Fig. 3a) for a frequency of 3000 rpm. Vibration stresses are imposed on the basic stresses and then are used in VHCF models for life duration estimations. The most dangerous area is shown in Fig. 3b.

# 3 Low Cycle Fatigue Models

## *3.1 LCF Models Based on the Stress State Estimation*

The coefficients in criteria of fatigue fracture are determined from the experiments for uniaxial cyclic loading for different values of stress ratio $R = \sigma_{\min}/\sigma_{\max}$, where $\sigma_{\max}$ and $\sigma_{\min}$ are the maximum and minimum stresses during the cycle. These values are used to define the stress amplitude $\sigma_a = (\sigma_{\max} - \sigma_{\min})/2$. In the case of uniaxial deformation, the test data are described using Wohler curves, which can be analytically written by using the Basquin formula [4]:

$$\sigma = \sigma_u + \sigma_c N^{\beta} \tag{1}$$

Here $\sigma_u$ is the fatigue limit, $\sigma_c$ is the fatigue strength factor, $\beta$ is the fatigue strength exponent, and $N$ is the number of cycles to fracture. A typical amplitude fatigue curve is depicted in Fig. 4. The curve consists of two branches corresponding to two fatigue regimes, the low cycle fatigue regime with fatigue limit $\sigma_u$ and very high cycle fatique regime with fatigue limit $\tilde{\sigma}_u$. The regime of interest is located in the left branch of the curve for life duration $N < 10^7$ cycles. The problem of fatigue fracture is that the spatial function of the life duration distribution $N$ must be determined from equations in the form (1) generalized to multi-axis stress state and containing the calculated stresses for the structure under study. Below the basic methods of generalizing the results of uniaxial tests to multi-axis stress state are considered [4].

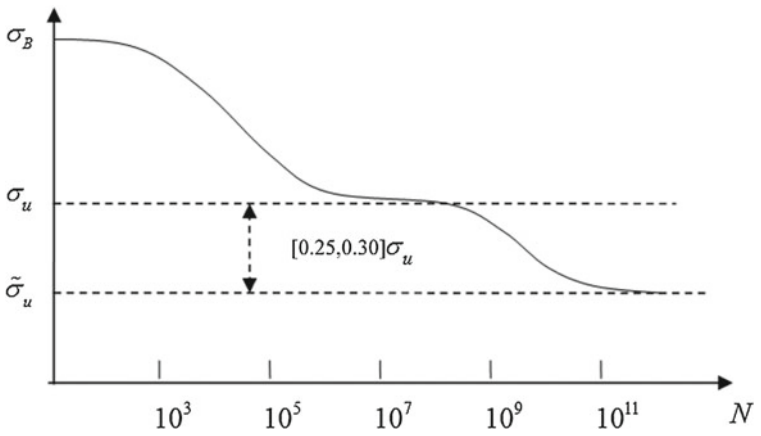


**Fig. 4** Typical fatigue Wohler's curve for metals. Here $\sigma_B$ is the strength limit, $\sigma_u$ and $\tilde{\sigma}_u$ are fatigue limits for LCF and VHCF regimes respectively

### 3.1.1 Sines Model

According to Sines [11], the uniaxial fatigue curve (1) may be generalized to multi-axis stress state as

$$\Delta\tau/2 + \alpha_s \sigma_{\text{mean}} = S_0 + AN^{\beta} \tag{2}$$

where

$$\sigma_{\text{mean}} = (\sigma_1 + \sigma_2 + \sigma_3)_{\text{mean}}$$
$$\Delta\tau = \sqrt{(\Delta\sigma_1 - \Delta\sigma_2)^2 + (\Delta\sigma_1 - \Delta\sigma_3)^2 + (\Delta\sigma_2 - \Delta\sigma_3)^2}/3$$

Here the parameter $\sigma_{\text{mean}}$ is the mean stress over a loading cycle. The parameter $\Delta\tau$ is the change in the octahedral tangent stress per cycle. The parameter $\Delta\tau/2$ is the octahedral tangent stress amplitude. Parameters $\alpha_s$, $S_0$, $A$ and $\beta$ are experimental. The model parameters for uniaxial fatigue curves are determined in [4]:

$$S_0 = \sqrt{2}\sigma_u/3, \quad A = 10^{-3\beta}\sqrt{2}(\sigma_B - \sigma_u)/3$$
$$\alpha_s = \sqrt{2}(2k_{-1} - 1)/3, \quad k_{-1} = \sigma_u/(2\sigma_{u0})$$

Here $\sigma_u$ and $\sigma_{u0}$ are the fatigue limits according to fatigue curves for $R = -1$ and $R = 0$, $N \approx 10^7 - 10^8$ cycles. It is assumed that the decrease of strength limit $\sigma_B$ is negligible up to the values $N \approx 10^3$ (Fig. 4).

### 3.1.2 Crossland Model

According to Crossland [5], the uniaxial fatigue curve (1) may be generalized to multi-axis stress state as

$$\Delta\tau/2 + \alpha_c(\overline{\sigma}_{\max} - \Delta\tau/2) = S_0 + AN^{\beta}, \quad \overline{\sigma}_{\max} = (\sigma_1 + \sigma_2 + \sigma_3)_{\max} \tag{3}$$

Here $\overline{\sigma}_{\max}$ is the maximum sum of principal stresses in a loading cycle, and $\alpha_c$, $S_0$, $A$ and $\beta$ parameters determined from experimental data. The final expressions for model parameters of the multiaxial model are determined in [4] for $R = -1$ and $R = 0$ as

$$S_0 = \sigma_u\left[\sqrt{2}/3 + (1 - \sqrt{2}/3)\alpha_c\right]$$
$$A = 10^{-3\beta}\left[\sqrt{2}/3 + (1 - \sqrt{2}/3)\alpha_c\right](\sigma_B - \sigma_u)$$
$$\alpha_c = (k_{-1}\sqrt{2}/3 - \sqrt{2}/6)\Big/\left[(1 - \sqrt{2}/6) - k_{-1}(1 - \sqrt{2}/3)\right]$$
$$k_{-1} = \sigma_u/(2\sigma_{u0})$$

### 3.1.3 Findley Model

The form of this model for the multi-axis stress state is proposed by Findley [7]

$$(\Delta\tau_s/2 + \alpha_F\sigma_n)_{\max} = S_0 + AN^{\beta} \tag{4}$$

Here $\tau_s$ and $\sigma_n$ are the absolute magnitudes of tangent stress and normal stress for the plane with normal vector $n_i$. For this plane, the combination $\Delta\tau_s/2+\alpha_F\sigma_n$ takes a maximum value. The model parameters are

$$S_0 = \sigma_u\left(\sqrt{1+\alpha_F{}^2}+\alpha_F\right)/2,$$
$$A = 10^{-3\beta}(\sqrt{1+\alpha_F{}^2}+\alpha_F)(\sigma_B-\sigma_u)/2$$
$$\alpha_F = \left[\sqrt{5k_{-1}{}^2-2k_{-1}}/2-k_{-1}(1-k_{-1})\right]\left[k_{-1}(2-k_{-1})\right]^{-1}$$

Approximate parameter values for the titanium alloy Ti-6Al-4V [4] (which are used in the computational example considered below) are limit strength of $\sigma_B = 1100$ MPa, fatigue limits based on $\sigma_a(N)$ amplitude curves for $R = -1$ and $R = 0$ of $\sigma_u = 450$ MPa and $\sigma_{u0} = 350$ MPa, exponent in the power-law dependence on the number of cycles of $\beta = -0.45$, Young's modulus of $E = 116$ GPa, shear modulus of $G = 44$ GPa, and Poisson's ratio of $\nu = 0.32$.

## *3.2 LCF Models Based on the Strain State Estimation*

Classical Coffin-Manson relation [10] describing uniaxial fatigue fracture on the basis of deformations is

$$\Delta\varepsilon/2 = (2N)^b\sigma_c/E + \varepsilon_c(2N)^c$$

Here $\sigma_c$ is the (axial) fatigue strength coefficient, $\varepsilon_c$ is the (axial) fatigue plasticity coefficient, $b$ and $c$ are the fatigue strength and fatigue plasticity exponents. Models generalizing the Coffin-Manson relation to the case of multi-axis fatigue fracture are briefly outlined below.

### 3.2.1 Brown-Miller Model

This model is proposed by Brown and Miller [2]; it takes into account the influence of tensile strains at the plane of maximum shear strain:

$$\frac{\Delta\gamma_{\max}}{2} + \alpha_{bm}\Delta\varepsilon_{\perp} = \beta_1\frac{\sigma_c - 2\sigma_{\perp\text{mean}}}{E}(2N)^b + \beta_2\varepsilon_c(2N)^c \tag{5}$$

Here $\gamma_{ij} = 2\varepsilon_{ij}$, $\varepsilon_{ij}$ are the strain tensor components; $\Delta\gamma_{\max}/2$ is the range of the maximum shear strains attained on the plane; $\Delta\varepsilon_{\perp}$ is the range of the tensile strains on this plane, and $\sigma_{\perp\text{mean}}$ is the cycle-average tensile stress on this plane. Approximate values for the coefficients are provided in [**?** ]: $\alpha_{bm} = 0.3$, $\beta_1 = (1+\nu)+(1-\nu)\alpha_{bm}$, $\beta_2 = 1.5 + 0.5\alpha_{bm}$.

### 3.2.2 Fatemi-Socie Model

This model is proposed by Fatemi and Socie [6]; it takes into account the influence of the normal stresses at the plane of maximum shear strains:

$$\frac{\Delta\gamma_{\max}}{2}(1 + k\frac{\sigma_{\perp\,\max}}{\sigma_y}) = \frac{\tau_c}{G}(2N)^{b_0} + \gamma_c(2N)^{c_0} \tag{6}$$

Here $\sigma_{\perp\,\max}$ is the cycle-maximum normal stress on the plane where $\gamma_{\max}$ is attained, $\sigma_y$ is the material yield strength, $\tau_c$ is the fatigue (shear) strength coefficient, $\gamma_c$ is the fatigue (shear) plasticity coefficient, $b_0$ and $c_0$ are the fatigue strength and fatigue plasticity exponents. The coefficient $k$ is approximately equal to $k = 0.5$ [4].

### 3.2.3 Smith-Watson-Topper Model

This model is described in [12] and accounts for the influence of the normal stress at the plane of maximum tensile strain:

$$\frac{\Delta\varepsilon_1}{2}\sigma_{\perp 1\,\max} = \frac{{\sigma_c}^2}{E}(2N)^{2b} + \sigma_c\varepsilon_c(2N)^{b+c} \tag{7}$$

Here $\Delta\varepsilon_1$ is the change in the maximum principal strain per cycle and $\sigma_{\perp 1\,\max}$ is the maximum normal stress at the plane of maximum tensile strain. The fatigue parameters for titanium alloys for this class of models are selected based on experimental data [4]: $\sigma_c = 1445$ MPa, $\varepsilon_c = 0.35$, $b = -0.095$, $c = -0.69$, $\tau_c = 835$ MPa, $\gamma_c = 0.20$, $b_0 = -0.095$, $c_0 = -0.69$, $\sigma_y = 910$ MPa.

## *3.3 LCF Models Based on Damage Estimation*

### 3.3.1 Lemaitre-Chaboche Model

The differential equation for damage D accumulated under multi-axis cyclic loading is proposed in [8] and after integration may be written as

$$N = \frac{1}{(1+\beta)a_M}\left[\frac{(1-3b_2\overline{\sigma})}{A_{IIa}}\right]^{\beta}\left\langle\frac{(\sigma_u - \sigma_{VM})}{(A_{IIa} - A^*)}\right\rangle \tag{8}$$

Here the notation from [8] is used

$$A_{IIa} = 0.5\sqrt{1.5\left(S_{ij,\max} - S_{ij,\min}\right)\left(S_{ij,\max} - S_{ij,\min}\right)}$$
$$\sigma_{VM} = \sqrt{0.5 S_{ij,\max} S_{ij,\max}}$$
$$\overline{\sigma} = (\sigma_1 + \sigma_2 + \sigma_3)_{\text{mean}}/3$$
$$A^* = \sigma_{10}\left(1 - 3b_1\overline{\sigma}\right)$$
$$a_M = a/M_0^{\beta}$$

The parameters $S_{ij,\max}$ and $S_{ij,\min}$ are maximum and minimum values of stress deviator during loading cycle; the angle brackets are defined as: $\langle X\rangle = 0$ for $X < 0$ and $\langle X\rangle = X$ for $X \geq 0$. The model parameters for a titanium alloy are given in [8]: $\beta = 7.689$, $b_1 = 0.0012$, $b_2 = 0.00085$ 1/MPa, $a_M = 4.1 \times 10^{-28}$, $\sigma_{10} = 395$ MPa, and $\sigma_u = 1085$ MPa.

### 3.3.2 The Liege University (LU) Model

This model is proposed and validated in [6]. In this case, the integrated differential equation for the damage is

$$N = \frac{\gamma + 1}{C}\left\langle \frac{\sigma_u - \theta \cdot \sigma_{VM}}{A_{IIa} - A^*} \right\rangle f_{\text{cr}}^{-(\gamma+1)} \tag{9}$$

Here the notation from [8] is used

$$f_{\text{cr}} = \frac{1}{b}\left(A_{IIa} + a\sigma_H - b\right), \quad f_{\text{cr}} > 0$$
$$A^* = \sigma_{-1}\left(1 - 3s\sigma_H\right)$$
$$\sigma_H = (\sigma_1 + \sigma_2 + \sigma_3)_{\max}/3$$

The model parameters are taken from [8]: $a = 0.467$, $b = 220$ MPa, $\gamma = 0.572$, $C = 7.12 \times 10^{-5}$, $\theta = 0.75$, $s = 0.00105$ 1/MPa, $\sigma_{-1} = 350$ MPa, $\sigma_u = 1199$ MPa.

## *3.4 Results of LCF Calculations*

As an example, we consider the problem of fatigue fracture of GTE compressor disks under low-cycle-fatigue (LCF) conditions. For each FLC (flight loading cycle) it is assumed that maximal loads and rotation correspond to cruising speed of aircraft. The problem is to calculate the life duration of the disk (N—the number of FLCs before fracture) from relations (2)–(9). To this end, it is necessary to calculate the stress state of the contact system of the compressor disk and blades under the combined action of centrifugal, aerodynamic and contact loads.

The input parameters include the angular velocity of rotation $\omega = 314$ rad/s (3000 rpm), the dynamic pressure at infinity $\rho v_\infty^2/2 = 26000$ N/m$^2$, corresponding to a flow velocity of 200 m/s and the air density of 1.3 kg/m$^3$. The total number of finite elements does not exceed 1,00,000 making it possible to solve the problem using usual personal computer. The material properties are $E = 116$ GPa, $\nu = 0.32$, and $\rho = 4370$ kg/m$^3$ for the disk (titanium alloy), $E = 69$ GPa, $\nu = 0.33$ and $\rho = 2700$ kg/m$^3$ for the blades and blade shroud ring (aluminum alloy), and $E = 207$ GPa, $\nu = 0.27$ and $\rho = 7860$ kg/m$^3$ for the fixing pins (steel).

The computations [3] indicate that the most dangerous areas are situated in the contact area of dovetail-type between the disk and the blades. The computations [3] also indicate that the best correspondence of computational and experimental data for stress concentration is provided when the detachment and slip of contacting elements (disk and blades) are taken into account. At the fixing pins boundary (Fig. 2b) the conditions of complete adhesion are used according to technological considerations. The zone of maximum tensile stress concentration is situated in the left (rounded) corner of the contact area of dovetail-type (Fig. 3b). The stress concentration is increased from the front to the rear portion of the groove according to observable nucleation of fatigue failure in the rear portion of the disk [10].

### *3.5 Estimate of Service Life for Structure Elements According to LCF Criteria*

In Fig. 5a–h, the computed number of flight cycles before fracture N for the chosen criteria and multi-axis models of fatigue fracture are displayed for the left corner of disk-blade contact joint of dovetail-type (in the zones of maximum stress concentration). The boundary of contact zone near the left corner of the groove is depicted by solid line (Fig. 6).

In Fig. 5a–h, the horizontal axis represents the dimensionless coordinate of the rounding of the groove's left corner; the vertical axis represents the dimensionless coordinate across the groove depth. The Sines, Lemaitre-Chaboche, Brown-Miller, and Smith-Watson-Topper criteria provide estimates for the service life of gas turbine engine disks of approximately 20,000–50,000 cycles. The Crossland and LU criteria predict the possibility of fatigue fracture after fewer than 20,000 flight cycles. On the whole, all of the criteria predict similar locations for the fatigue fracture regions. The Fatemi-Socie criterion gives a service life prediction of approximately 1,00,000 cycles. The deviation of the Fatemi-Socie estimate from the results based on the other criteria suggests that the shear mechanism of multi-axis fatigue fracture, which is reflected in this criterion, is not purely realized in flight loading. Remark that 25,000 flight cycles correspond to an in-service lifetime of 50,000 h for two hour flights.

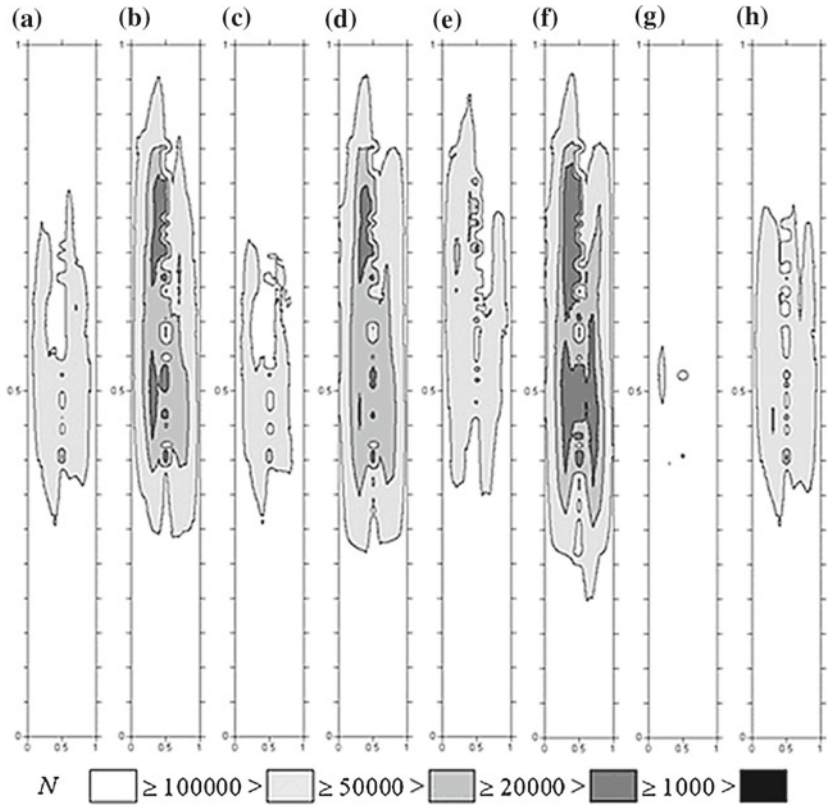


**Fig. 5** Life duration estimates in the area of failure initiation for LCF models: **a** Sines, **b** Crossland, **c** Findley, **d** Brown-Miller, **e** Fatemi-Socie, **f** Smith-Watson-Topper, **g** Lemaitre-Chaboche, **h** Liege University

**Fig. 6** The area of failure initiation; it is indicated by *solid lines* and situated in the slot of dovetail-type connection

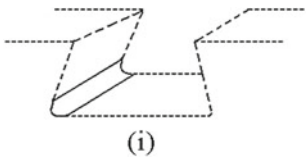


## 4 Very High Cycle Fatigue Models

An alternative fatigue mechanism may also be examined for high frequency axial vibrations of the shroud ring. The amplitude of vibrations and stress state disturbances near stress concentrators are relatively small, but the number of high frequency vibrations can be as high as $10^9-10^{10}$, and evaluation of the very-high-cycle fatigue (VHCF) regime is necessary because fatigue may take place even if stress levels are below classical fatigue limits [7]. At present there is no experimentally verified

multi-axis VHCF theory for titanium alloy. In order to obtain life duration estimates the known multi-axis LCF models (2), (4), and (6) are used, taking into account general assumptions about VHCF curves. A typical fatigue curve is presented in Fig. 4, and in case of VHCF the right portion of the curve for $N > 10^8$ is of interest.

### 4.1 Generalization of Sines Model

The VHCF parameters are determined using one-dimensional fatigue curves in a manner similar to the LCF case. The similarity between the left and right halves of the fatigue curve is taken into account through the substitution $\sigma_B \to \sigma_u$, $\sigma_u \to \tilde{\sigma}_u$ and $\sigma_{u0} \to \tilde{\sigma}_{u0}$, where $\tilde{\sigma}_u$ and $\tilde{\sigma}_{u0}$ are new fatigue limits for right half of the fatigue curve for asymmetry factors $R = -1$ and $R = 0$, $N > 10^{11}$ cycles (Fig. 4). The VHCF parameter values for the generalized Sines model (2) are

$$S_0 = \sqrt{2}\tilde{\sigma}_u/3, \quad A = 10^{-8\beta}\sqrt{2}(\sigma_u - \tilde{\sigma}_u)/3,$$
$$\alpha_s = \sqrt{2}(2k_{-1} - 1)/3, \quad k_{-1} = \tilde{\sigma}_u/\tilde{\sigma}_{u0}/2$$

### 4.2 Generalization of Crossland Model

By analogy the VHCF parameters for the generalized Crossland model (4) are

$$S_0 = \tilde{\sigma}_u \left[\sqrt{2}/3 + (1 - \sqrt{2}/3)\alpha_c\right], \quad A = 10^{-8\beta}(\sigma_u - \tilde{\sigma}_u)\left[\sqrt{2}/3 + (1 - \sqrt{2}/3)\alpha_c\right]$$

### 4.3 Generalization of Findley Model

The VHCF parameters for the generalized Findley model (6) are

$$S_0 = \tilde{\sigma}_u \left(\sqrt{1 + \alpha_F{}^2} + \alpha_F\right)/2, \quad A = 10^{-8\beta}(\sigma_u - \tilde{\sigma}_u)(\sqrt{1 + \alpha_F{}^2} + \alpha_F)/2$$

For titanium alloy the following parameter values are used $\sigma_u = 450$ MPa, $\tilde{\sigma}_u = 250$ MPa, $\tilde{\sigma}_{u0} = 200$ MPa. $\beta = -0.3$

### 4.4 Results of VHCF Calculations

The maximum stress concentration occurs near the rounding of the groove's left corner. The calculated limits of $N$ (number of safe vibration cycles) for a selected

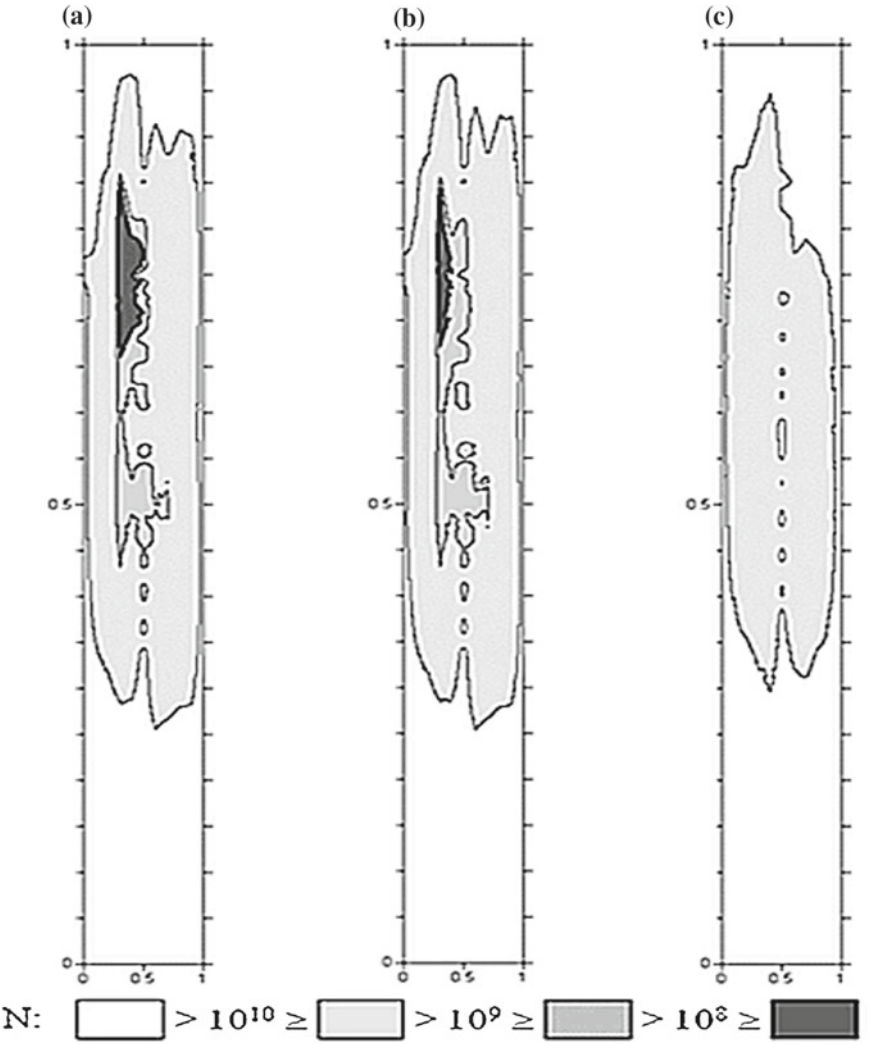


**Fig. 7** Life duration estimates in the area of failure initiation for VHCF models: **a** Sines, **b** Crossland, **c** Findley

area of the left corner are depicted in Fig. 7. The results were obtained using the VHCF generalized criteria of Sines, Crossland, and Findley. Despite the rather low additional vibration stress amplitude level in this case, zones of fatigue failure are also appeared. The fatigue failure zones are situated near the rear portion of the groove's left corner (in the same location as in the LCF case). The safe vibration loading cycle number is approximately equal to $10^9 - 10^{10}$, corresponding to an in-service lifetime of 50,000 h.

## 5 Conclusions

A numerical model is developed to estimate the service life of structural elements for both LCF (flight cycles) and VHCF (vibrations) regimes. Comparative estimates of life duration for GTE compressor disk-blade contact structures were obtained using Sines, Crossland, and Findley fatigue models. The life duration estimates obtained for LCF and VHCF mechanisms coincided closely with the observed service life of titanium compressor disks in the D30-KU-154 GTE. So, original and generalized fatigue failure criteria may be used for estimating in-service life duration of titanium disks.

Although presented life duration estimates are rather approximate, they highlight the possibility of fatigue fracture development in structural elements for both LCF (flight cycles) and VHCF (high frequency low amplitude vibrations) regimes. The most serious hazard may happen due to mutual action of the both mechanisms because they may cause the fatigue failure developed almost simultaneously and in the same location.

**Acknowledgments** The research was supported by the Russian Foundation for Basic Research under projects 15-08-02392-a.

## References

1. C. Bathias, P.C. Paris, *Gigacycle fatigue in mechanical practice* (Marcel Dekker Verlag, 2004)
2. M.W. Brown, K.J. Miller, A theory for fatigue failure under multiaxial stress-strain conditions. Proc. Inst. Mech. Eng. **187**(1), 745–755 (1973)
3. N.G. Burago, A.B. Zhuravlev, I.S. Nikitin, Analysis of stress state of the contact system "disc-blad". Comput. Contin. Mech. **4**(2), 5–16 (2011)
4. N.G. Burago, A.B. Zhuravlev, I.S. Nikitin, Models of multiaxial fatigue fracture and service life estimation of structural elements. Mech. Solids **46**(6) (2011)
5. B. Crossland, Effect of large hydrostatic pressures on the torsional fatigue strength of an alloy steel. In *Proceedings of the International Conference on Fatigue of Metals* (Institution of Mechanical Engineers, London, 1956), pp. 138–149
6. A. Fatemi, D.F. Socie, A critical plane approach to multiaxial fatigue damage including out-of-phase loading. Fatigue Fract. Eng. Mater. Struct. **11**(3), 149–165 (1988)
7. W.N. Findley, A theory for the effect of mean stress on fatigue of metals under combined torsion and axial load or bending. J. Eng. Ind. **81**(4), 301–306 (1959)
8. A.K. Marmi, A.M. Habraken, L. Duchene, Multiaxial fatigue damage modelling at macro scale of Ti-6Al-4V alloy. Int. J. Fatigue **31**(11–12), 2031–2040 (2009)
9. I.V. Papadopoulos, P. Davoli, C. Gorla, M. Filippini, A. Bernasconi, A comparative study of multiaxial high-cycle fatigue criteria for metals. Int. J. Fatigue **19**(3), 219–235 (1997)
10. A.A. Shanyavskiy, *Modeling of Metal Fatigue Fracture* (Monografiya, Ufa, 2007) (in Russian)
11. G. Sines, Behavior of metals under complex static and alternating stresses, in *Metal Fatigue*, ed. by G. Sines, J.L. Waisman (McGraw-Hill, New York, 1959), pp. 145–169
12. R.N. Smith, P. Watson, T.H. Topper, A stress-strain parameter for the fatigue of metals. J. Mater. **5**(4), 767–778 (1970)
13. Y.-Y. Wang, W.-X. Yao, Evaluation and comparison of several multiaxial fatigue criteria. Int. J. Fatigue **26**(1), 17–25 (2004)